Electronic Supplementary Material (ESI) for RSC Mechanochemistry.
This journal is © The Royal Society of Chemistry 2024

Supporting Information: Green-chemistry synthesis and optical properties of the lead-free $Cs_2AgSbCl_6$ double perovskite by the mechanochemical method

Karla K. F. Barbosa,[†] Deisy Aristizábal-Giraldo,[‡] José Javier S. Acuña,[†] Jorge M. Osorio-Guillén,[‡] and Fabio F. Ferreira[†]

†*Centro de Ciências Naturais e Humanas (CCNH), Universidade Federal do ABC (UFABC), Santo André, SP, 09210-580 Brazil*

‡*Instituto de Física, Universidad de Antioquia UdeA, Calle 70 No 52-21, Medellín, Colombia*

1 Materials and methods

Reagents

CsCl (Inlab Confiança, 99.9 %, 168.36 g mol^{-1}), AgCl (Alfa Aesar, 99.5 %, 143.32 g mol^{-1}), $SbCl_3$ (Alfa Aesar, 99 %, 228.12 $gmol^{-1}$), and HCl (Synth 38 wt% in water) were purchased and used as received without further purification. The amounts of reagents used in the synthesis of $Cs_2AgSbCl_6$ were as follows: CsCl (95.10 mg, 0.56 mmol), AgCl (40.48 mg, 0.28 mmol), and $SbCl_3$ (64.42 mg, 0.28 mmol).

Synthesis of the materials

The lead-free halide double perovskites were synthesized by grinding the precursors in an electric mixer mill (Retsch Mixer Mill MM−400) using 2 mL polypropylene microcentrifuge tubes and 4 agate balls (∅ =5 mm) (see Figure S1) following the same process described for Kubicki et al.[S1], but the polypropylene microcentrifuge tubes were placed into 5 mL stainless steel jars, from 2 min to 60 min at 30 Hz). The total mass of the precursors (0.2 g) was weighed and handled in a glove box with Ar 1200 ppm and O_2 12 % and inserted into each polypropylene microtube, with a molar ratio of 2:1:1 in relation to CsCl, AgCl, and $SbCl_3$, respectively. Before finishing the grinding process (about 5 min before), 1 μL of HCl was added to suppress the AgCl phase, and the rest of the grinding was completed. All samples were annealed for 12 h at 100 °C to remove milling-induced defects.

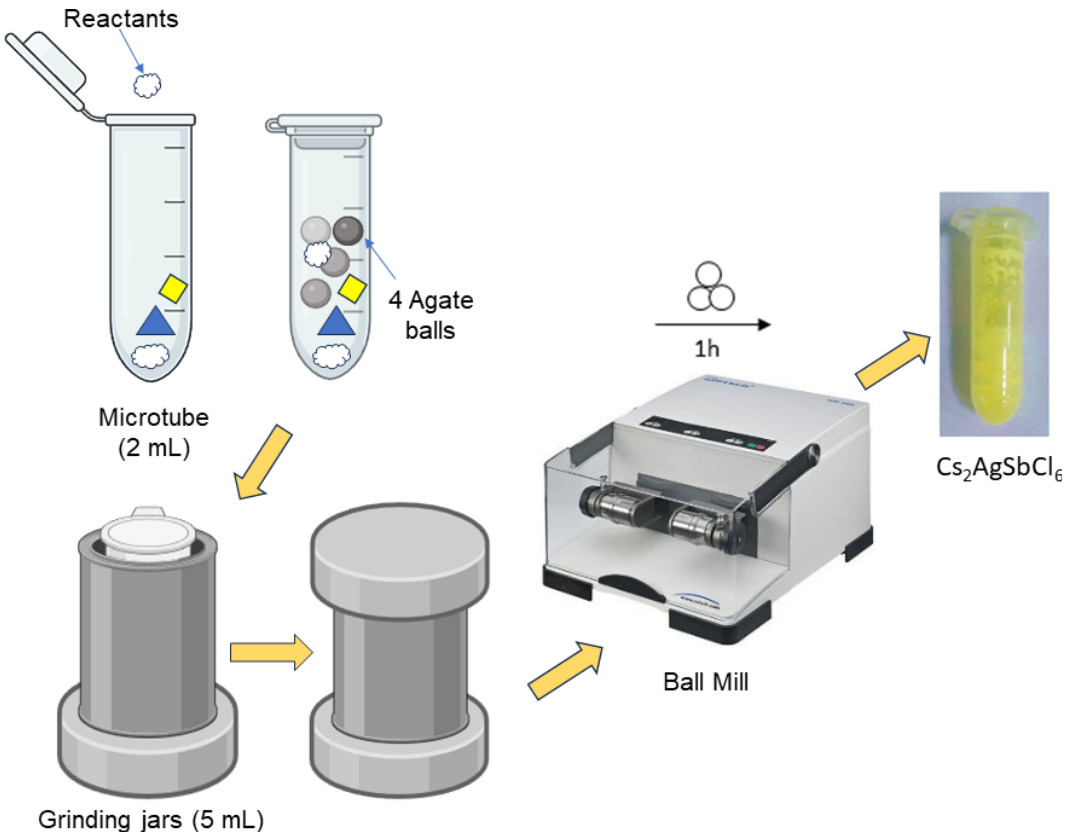

Figure S1 Illustration of the ball-milling process.

The role of solvent in mechanochemistry

Mechanochemical liquid-assisted grinding (LAG), an extension of conventional solvent-free mechanochemical techniques, involves the incorporation of a small amount of liquid as an additive to boost and/or regulate reactivity. This approach has successfully screened inclusion compounds, cocrystals, salts, solvates, and polymorphs[S2].

Motivated by Friščić et al.'s work in which the ratio between the volume of the liquid phase and the amount of solid present in each experiment is a concept used in the study of cocrystals[S3], we have used the same definition as the empirical η parameter, where V is the volume of solvent (in μL) divided by the sample mass (in mg). The latter represents the combination of all binary salts in the stoichiometric ratios described previously.

$$\eta = \frac{V \text{ (liquid, } \mu L)}{m \text{ (sample, } mg)}$$

Thus, the parameter η was varied ($0 \leqslant \eta \leqslant 0.005$) to investigate its effect on the synthesis, with HCl as a solvent assistant in griding.

Powder X-ray diffraction

The powder X-ray diffraction patterns of the reaction products for different milling times and their respective phases obtained by Rietveld refinements are displayed in Figures S2-S5.

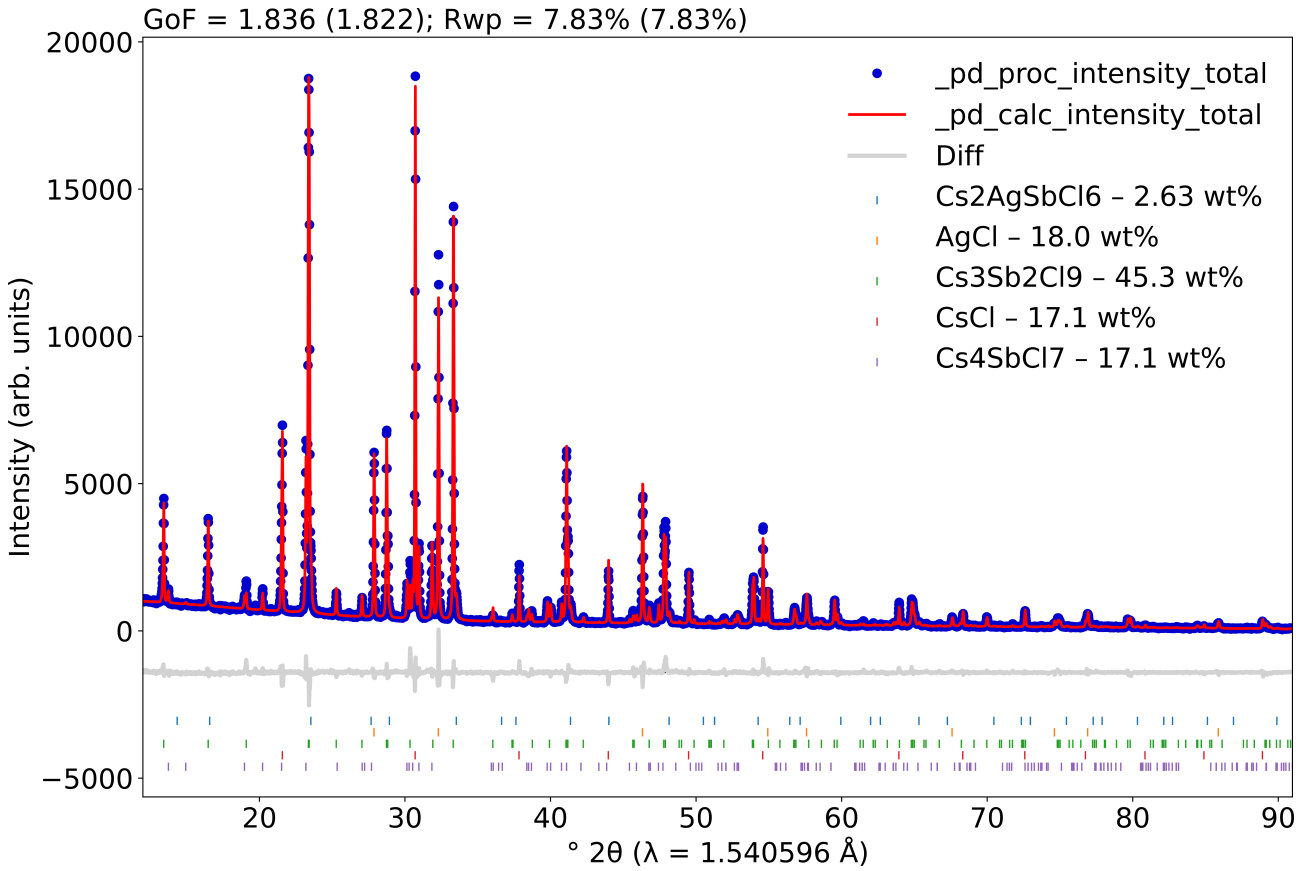

Figure S2 Rietveld plot of the double perovskite $Cs_2AgSbCl_6$, for t = 2 min. The observed pattern is represented by blue dots, while the calculated one is displayed in red line. The difference between the observed and calculated patterns is indicated by a gray line. The observed phases are indicated by vertical bars: $Cs_2AgSbCl_6$ (blue), CsCl (red), AgCl (orange), $Cs_3Sb_2Cl_9$ (green), and Cs_4SbCl_7 (purple). This graph was prepared using the pdCIFplotter program[S4].

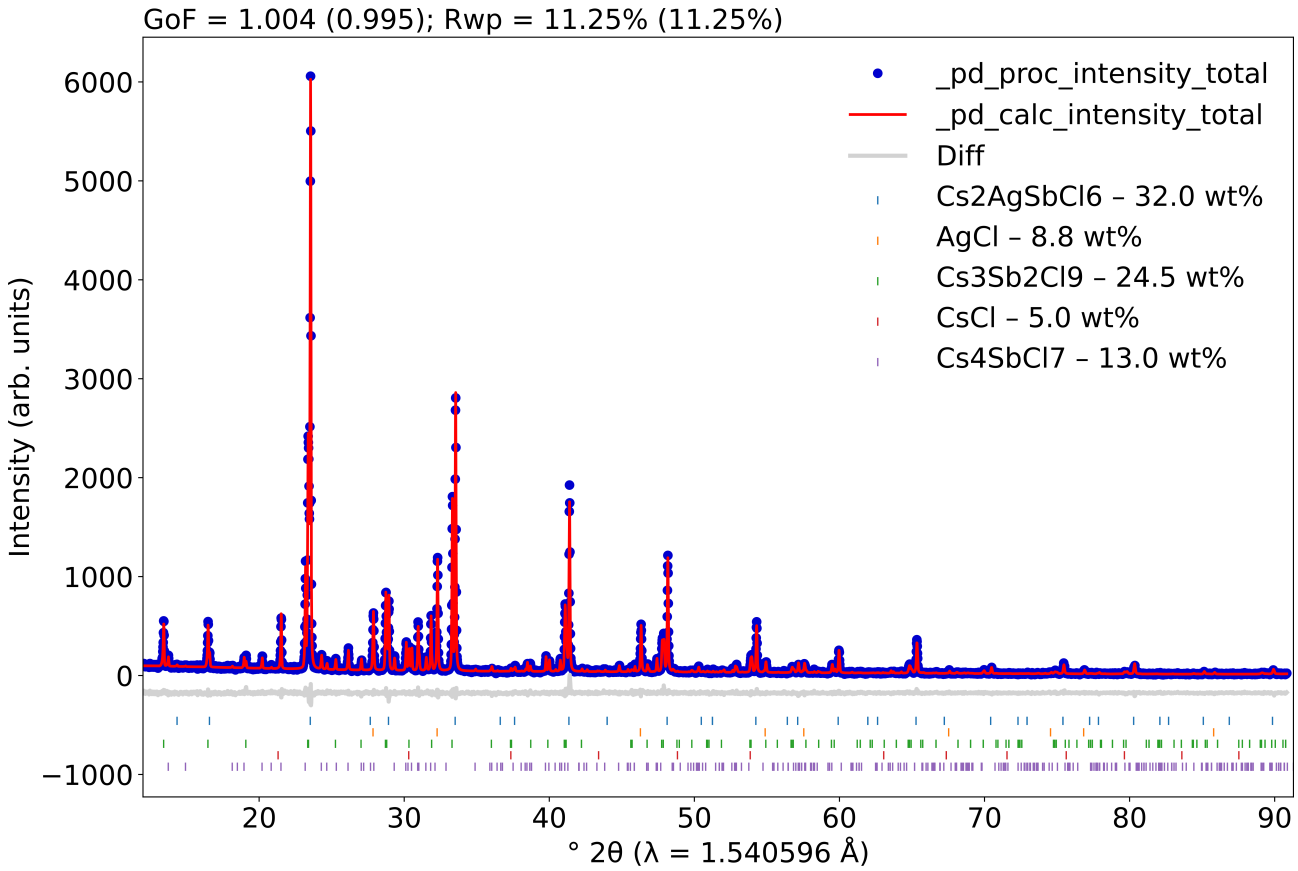

Figure S3 Rietveld plot of the double perovskite $Cs_2AgSbCl_6$, for t = 5 min. The observed pattern is represented by blue dots, while the calculated one is displayed in red line. The difference between the observed and calculated patterns is indicated by a gray line. The observed phases are indicated by vertical bars: $Cs_2AgSbCl_6$ (blue), CsCl (red), AgCl (orange), $Cs_3Sb_2Cl_9$ (green), and Cs_4SbCl_7 (purple). This graph was prepared using the pdCIFplotter program[S4].

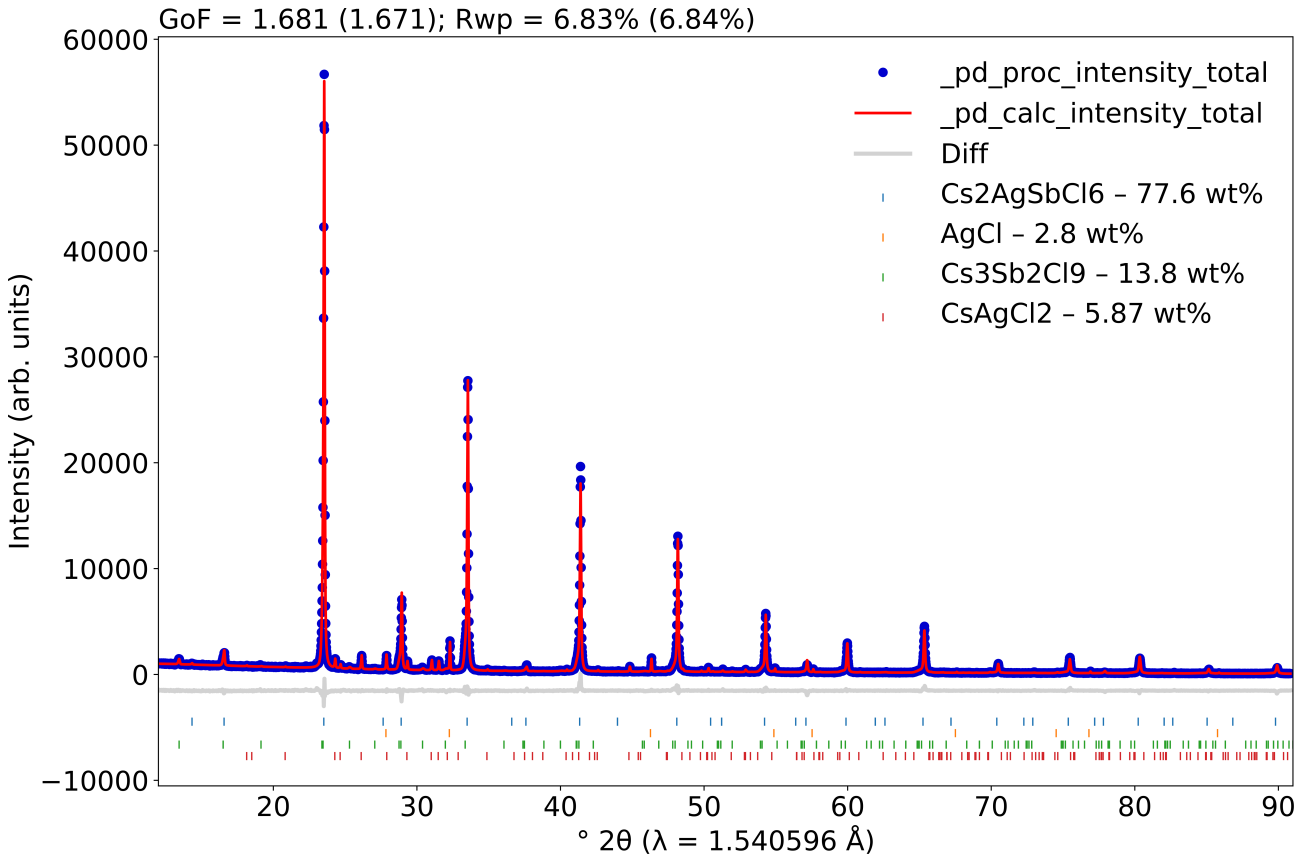

Figure S4 Rietveld plot of the double perovskite $Cs_2AgSbCl_6$, for t = 10 min. The observed pattern is represented by blue dots, while the calculated one is displayed in red line. The difference between the observed and calculated patterns is indicated by a gray line. The observed phases are indicated by vertical bars: $Cs_2AgSbCl_6$ (blue), AgCl (orange), $Cs_3Sb_2Cl_9$ (green), and $CsAgCl_2$ (red). This graph was prepared using the pdCIFplotter program[S4].

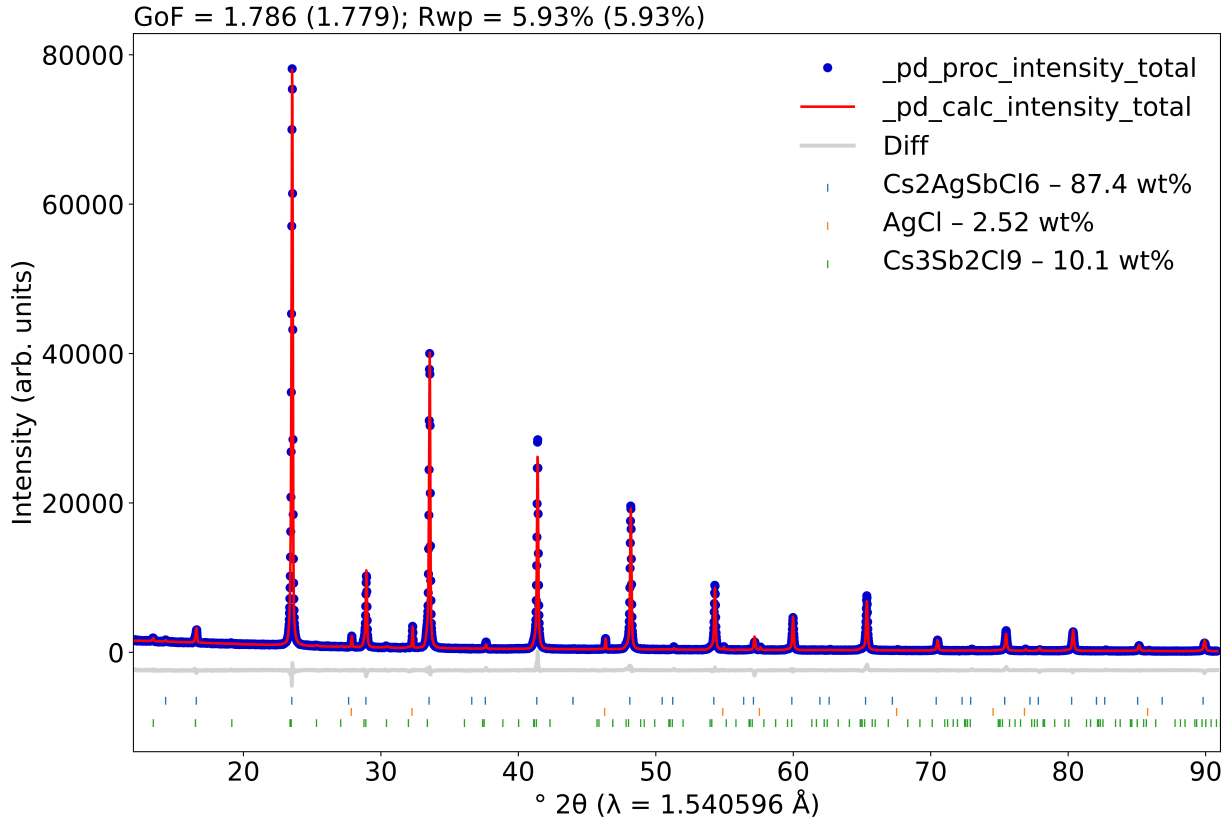

Figure S5 Rietveld plot of the double perovskite $Cs_2AgSbCl_6$, for t = 15 min. The observed pattern is represented by blue dots, while the calculated one is displayed in red line. The difference between the observed and calculated patterns is indicated by a gray line. The observed phases are indicated by vertical bars: $Cs_2AgSbCl_6$ (blue), AgCl (orange), and $Cs_3Sb_2Cl_9$ (green). This graph was prepared using the pdCIFplotter program[S4].

After 60 min, the minority AgCl and $Cs_3Sb_2Cl_9$ phases were persistent, so we added a drop of HCl to reduce them. This decision was taken since metallic AgCl was not integrated during grinding. Consequently, we introduced an amount of AgCl ($\eta = 0.1$) with 20 μL of HCl, a solvent commonly used to dissolve binary AgCl salts, CsCl, and $SbCl_3$. Unfortunately, the perovskite phase was not achieved. Two samples were subjected to the same test at 30 Hz for 1 h – one without adding HCl and the other with 1 μL of HCl – and their X-ray patterns are presented in Figures S6-S9. Subsequent attempts to nearly-dry grinding with a drop of HCl (1 μL) for the sole purpose of evaluating the incorporation evolution revealed that $\eta = 0.005$ would be the ideal value for enhancing the purity of the $Cs_2AgSbCl_6$ perovskite phase.

We inferred that adding HCl incorporates the $Cs_3Sb_2Cl_9$ phase into the perovskite, leading

to a decrease in observed AgCl. Further empirical evaluations involving additions exceeding 1 μL and up to 3 μL resulted in the perovskite phase formation. It is worth noting that these adjustments were conducted empirically, and no attempts were made using other solvents.

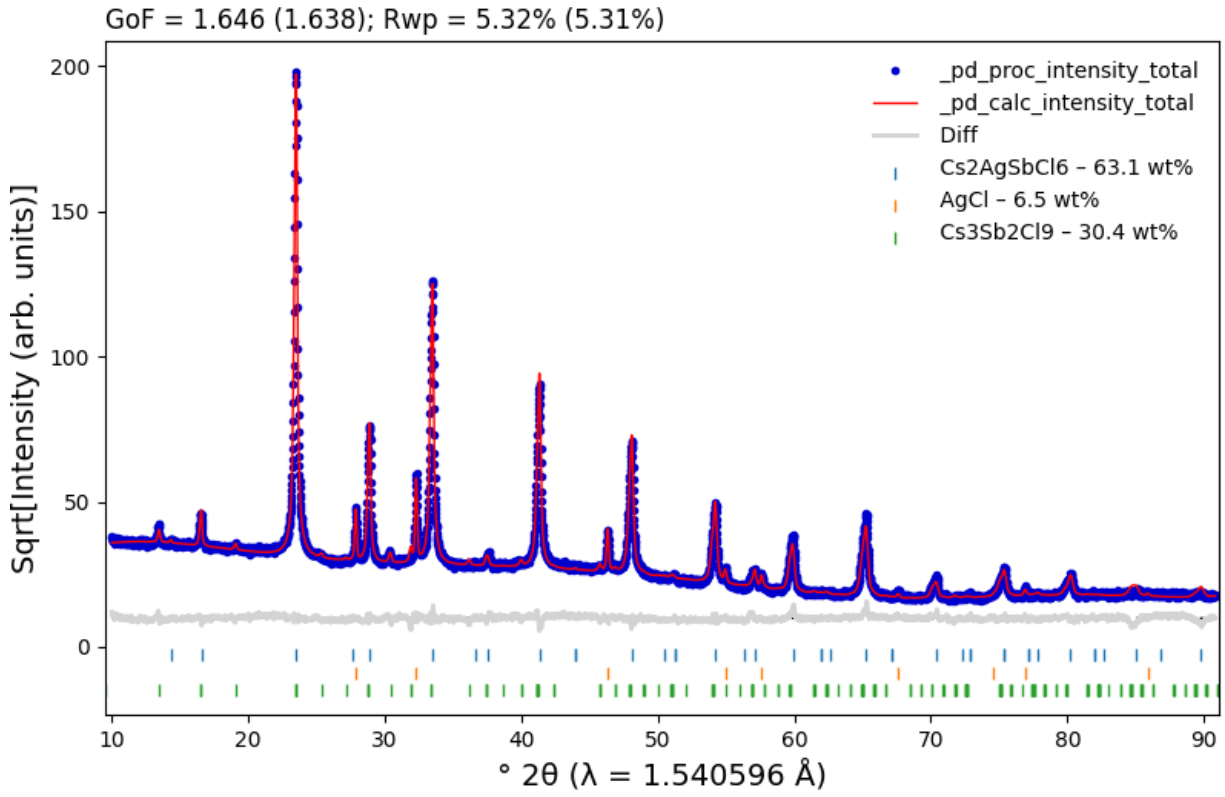

Figure S6 Rietveld plot of the double perovskite $Cs_2AgSbCl_6$ without the addition of HCl. The observed pattern is represented by blue dots, while the calculated one is displayed in red line. A gray line indicates the difference between the observed and calculated patterns. The observed phases are indicated by vertical bars: $Cs_2AgSbCl_6$ (blue), AgCl (orange), and $Cs_3Sb_2Cl_9$ (green). This graph was prepared using the pdCIFplotter program [S4]. The counts are represented as square roots for better visualization of low-intensity peaks.

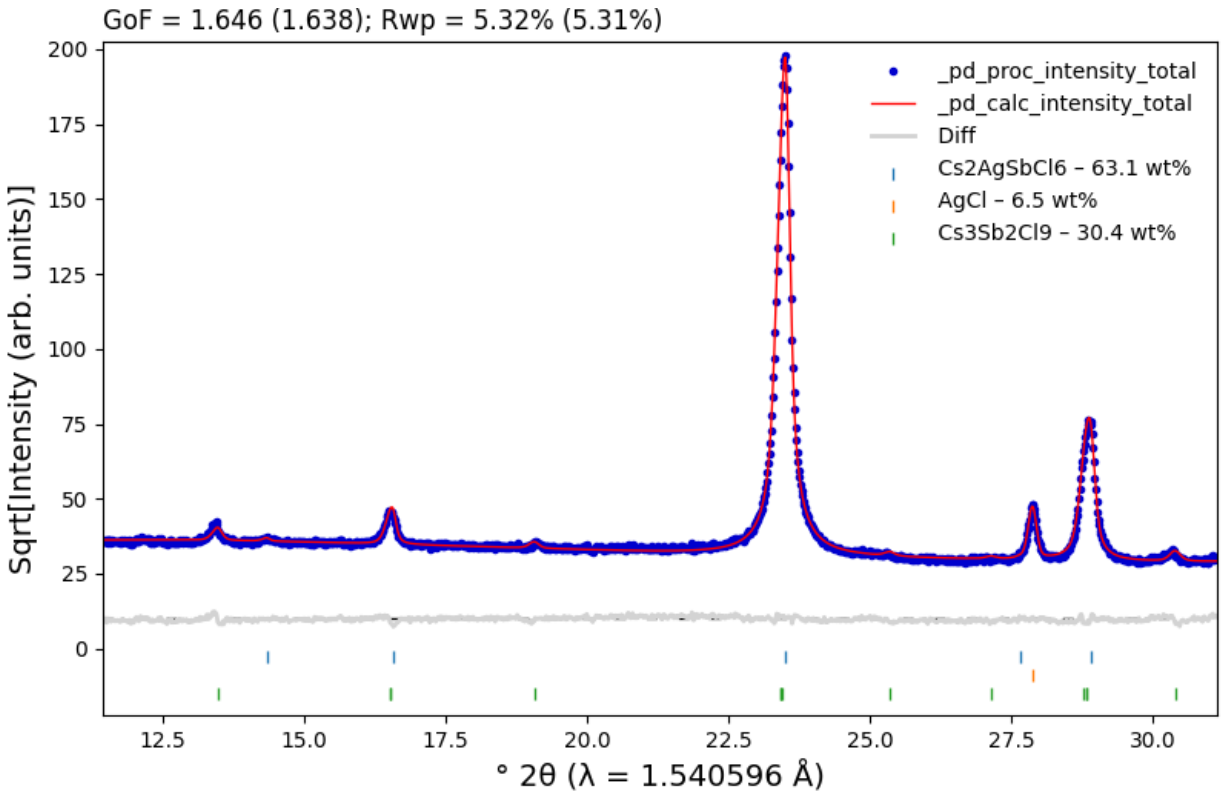

Figure S7 Rietveld plot of the double perovskite $Cs_2AgSbCl_6$ magnified in the region of 12° − 30° (2θ), highlighting the reflections regarding the $Cs_2AgSbCl_6$, $Cs_3SbCl_9$and AgCl phases without the addition of HCl. Blue dots represent the observed pattern, while the calculated one is displayed in red. A gray line indicates the difference between the observed and calculated patterns. The observed phases are indicated by vertical bars: $Cs_2AgSbCl_6$ (blue), AgCl (orange), and $Cs_3Sb_2Cl_9$ (green). This graph was prepared using the pdCIFplotter program [S4]. The counts are represented as square roots for better visualization of low-intensity peaks.

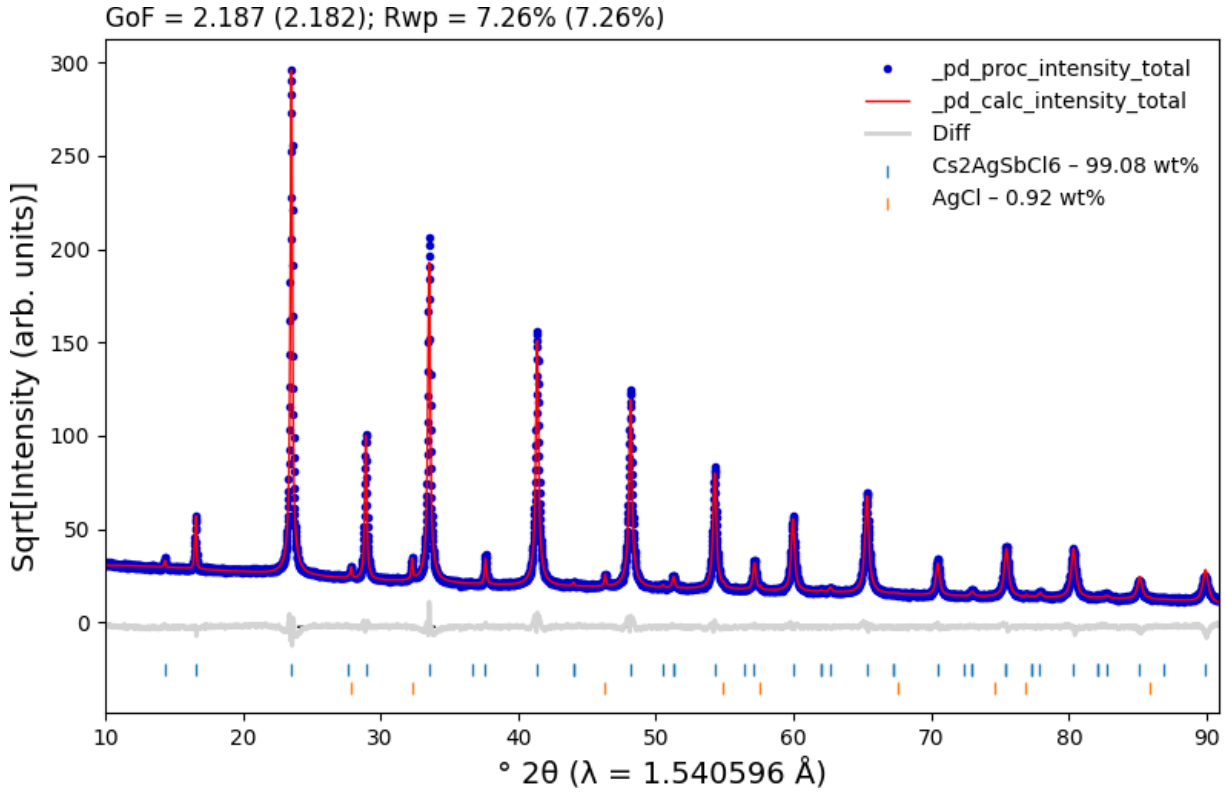

Figure S8 Rietveld plot of the double perovskite $Cs_2AgSbCl_6$ with the addition of HCl (1 μL). Blue dots represent the observed pattern, while the calculated one is displayed in red. A gray line indicates the difference between the observed and calculated patterns. The observed phases are indicated by vertical bars: $Cs_2AgSbCl_6$ (blue) and AgCl (orange). This graph was prepared using the pdCIFplotter program [S4]. The counts are represented as square roots for better visualization of low-intensity peaks.

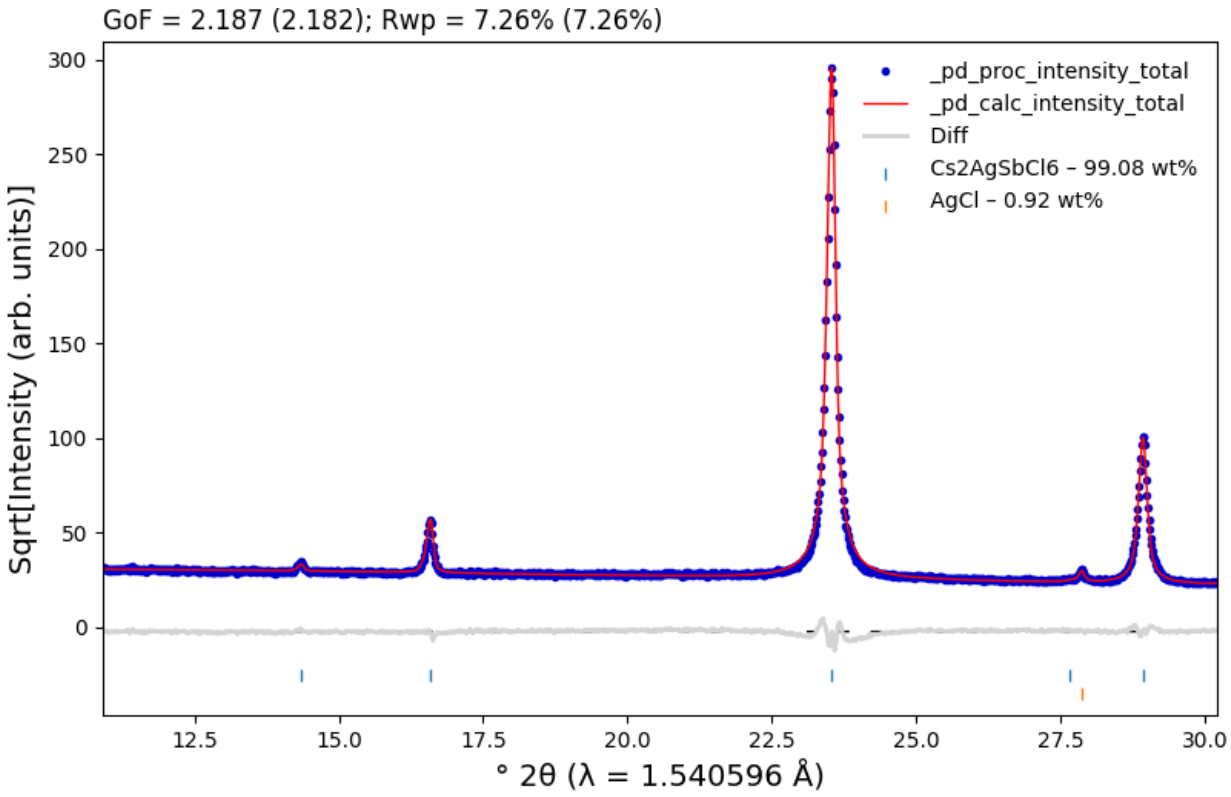

Figure S9 Rietveld plot of the double perovskite $Cs_2AgSbCl_6$, zoom in the region of 12° − 30° (2θ), highlighting the reflections regarding the $Cs_2AgSbCl_6$ and AgCl phases with the addition of HCl (1 μL). Blue dots represent the observed pattern, while the calculated one is displayed in red. A gray line indicates the difference between the observed and calculated patterns. The observed phases are indicated by vertical bars: $Cs_2AgSbCl_6$ (blue) and AgCl (orange). This graph was prepared using the pdCIFplotter program [S4]. The counts are represented as square roots for better visualization of low-intensity peaks.

After 365 days, we carried out another measurement of the mechanoperovskite powder and it was possible to verify the structural stability of the compound (See Figure S10; however, its color changed from yellow to pale yellow.

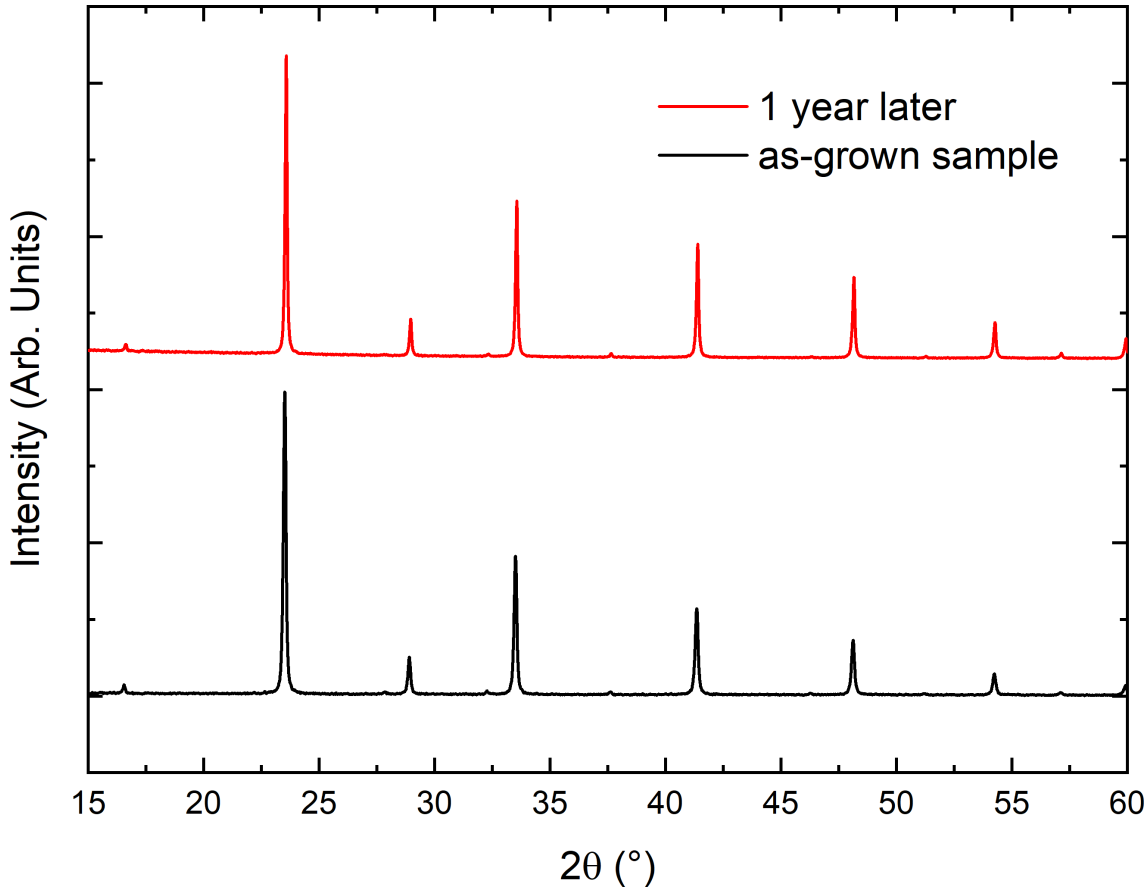

Figure S10 PXRD diffraction patterns measured for the double perovskite $Cs_2AgSbCl_6$ for as-grown (black line) and one year later (red line), $\lambda = 1.540596$ Å**.**

SEM measurements

Using scanning electron microscopy (SEM) to demonstrate that despite the non-uniformity of particles, the characteristic homogeneity is demonstrated by SEM mapping (see Figure S11) combined with Energy-dispersive X-ray spectrometer, EDS spectra of the Cs2AgSbCl crystalline phase demonstrate good agreement of the starting precursors (see Figure S12).

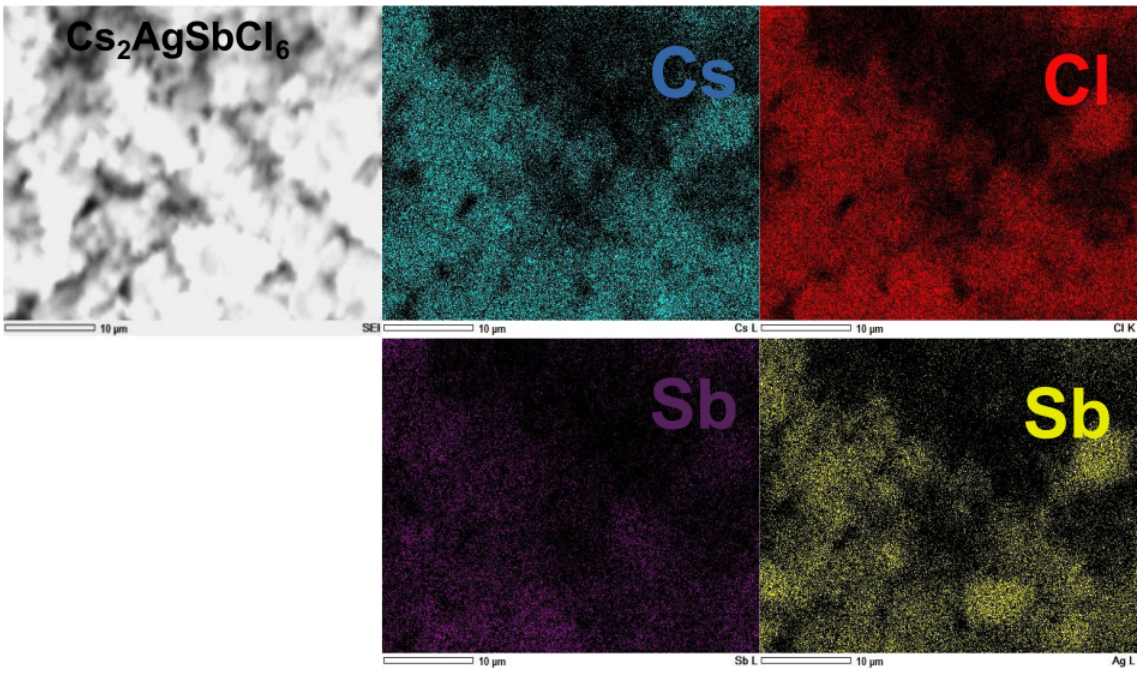

Figure S11 Elemental distribution map (energy-dispersive X-ray spectroscopy using a scanning electron microscope, SEM-EDX) of the mechanochemically synthesized $Cs_2AgSbCl_6$ particles.

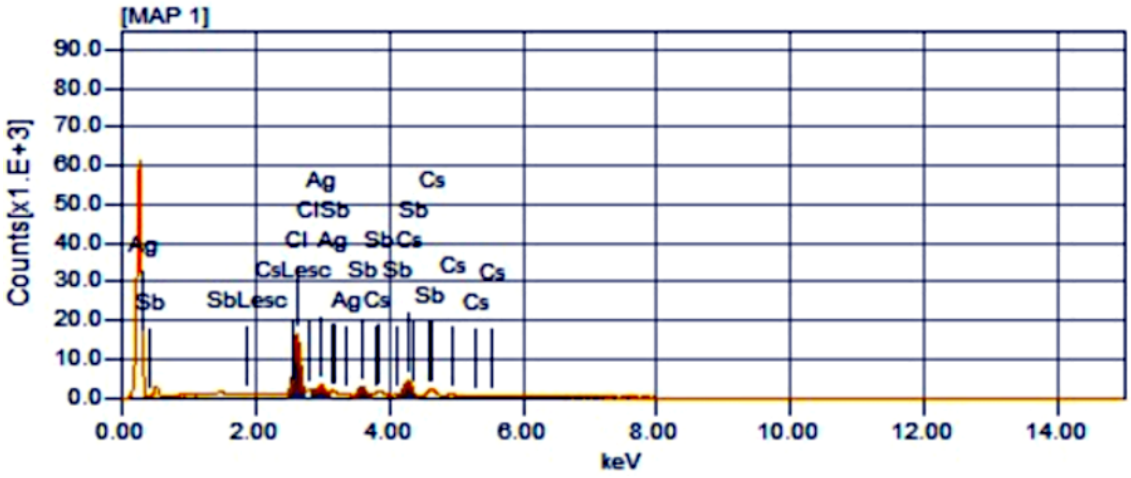

Figure S12 Diagram showing EDX spectra from $Cs_2AgSbCl_6$ perovskite powder.

HRTEM measurements

CASC powders were completely dissolved in 5 mL DMSO, forming a transparent solution, following the ligand-assisted reprecipitation (LARP) technique[S5]. After that, 0.5 mL of precursors were injected into the 10 mL ethyl acetate solution under vigorous stirring at room temperature. To synthesize oleic acid (OA)-capped NPs, 0.4 mL of OA was added to the antisolvent.

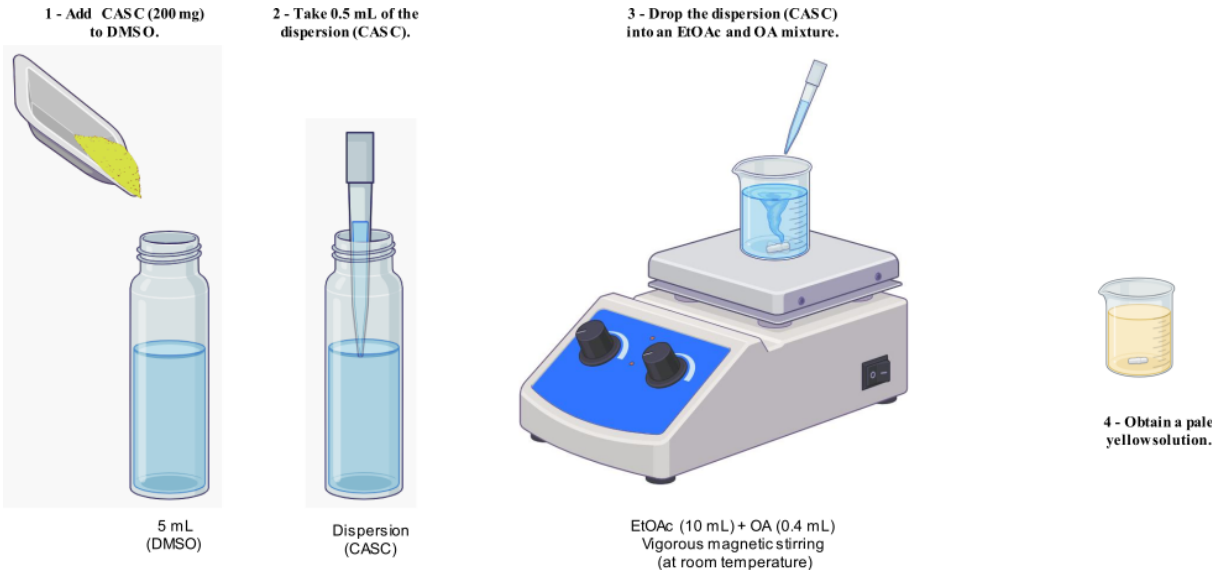

Figure S13 Scheme of the dispersion for the double perovskite $Cs_2AgSbCl_6$.

The preparation of these $Cs_2AgSbCl_6$ samples follows the following steps:

1. The mechanoperovskite solution was centrifuged at 5000 rpm for 5 minutes, and the precipitate was collected and supernatant discarded;

2. The sample was washed with octane and acetone 1:1 to eliminate some impurities from the dissolution, followed by centrifugation at 8000 rpm for 5 minutes; a white precipitated powder was collected, and the supernatant discarded. This washing was performed twice;

3. Approximately 4 mg of the powder was dispersed into 1 mL of hexane and then subjected

to sonication to promote nanoparticle dispersion. A pale-white solution was obtained after 10 minutes;

4. Using a pipette, we dropped 1 μL of the supernatant onto the TEM grid.

Before obtaining the HRTEM images, we performed a PXRD measurement to confirm that dispersing CASC particles does not change the perovskite structure (see Figure S14).

The dispersed solution process did not change the perovskite structure, but the $CsAgCl_2$ phase can be observed in the Rietveld refinement.

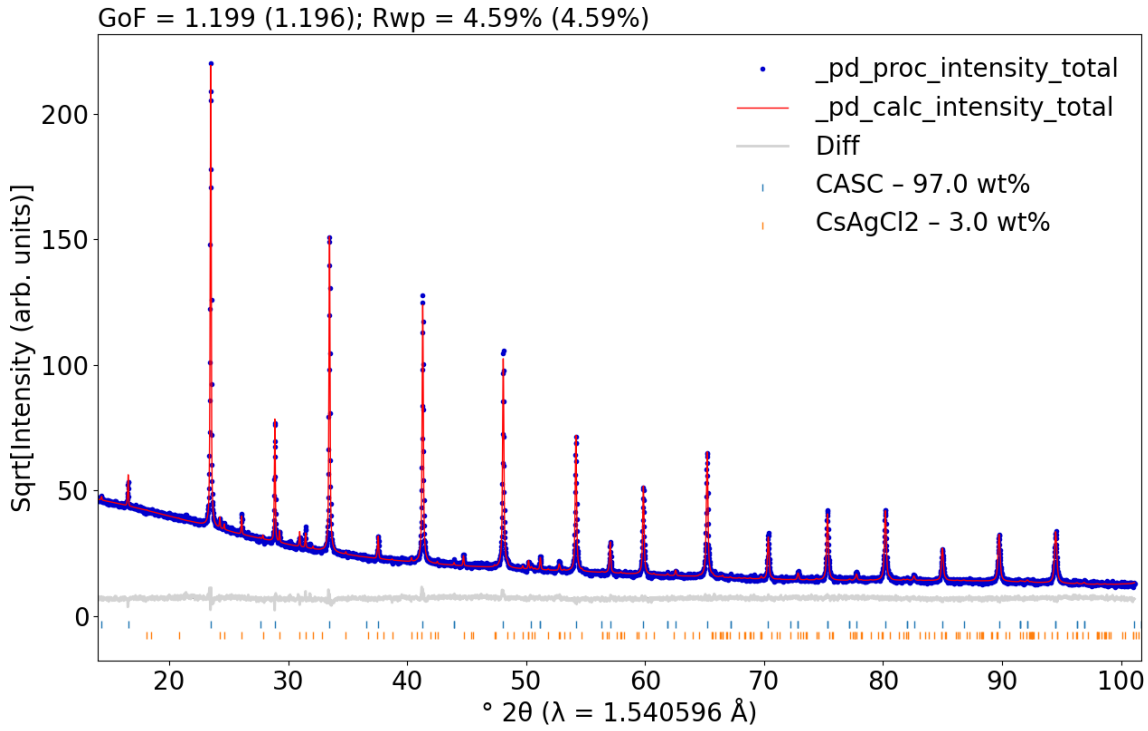

Figure S14 Rietveld plot of the double perovskite $Cs_2AgSbCl_6$ obtained from a solution. Blue dots represent the observed pattern, while the calculated one is displayed in the red line. A gray line indicates the difference between the observed and calculated patterns. The observed phases are indicated by vertical bars: $Cs_2AgSbCl_6$ (blue) and $CsAgCl_2$ (orange). This graph was prepared using the pdCIFplotter program [S4]. The counts are represented as square roots for better visualization of low-intensity peaks.

UV-Vis measurements

The optical band gap of CASC is 2.61(3) eV. It was obtained from the linear fitting of the absorption spectra and the Tauc plot when the reflectance, R, is transformed following the Kubelka-Munk[S6] equation:

$$F(R) = \frac{(1-R)^2}{2R}$$

The linear fit of the relationship vs. energy, the energy gap, was determined by interception on the x-axis.

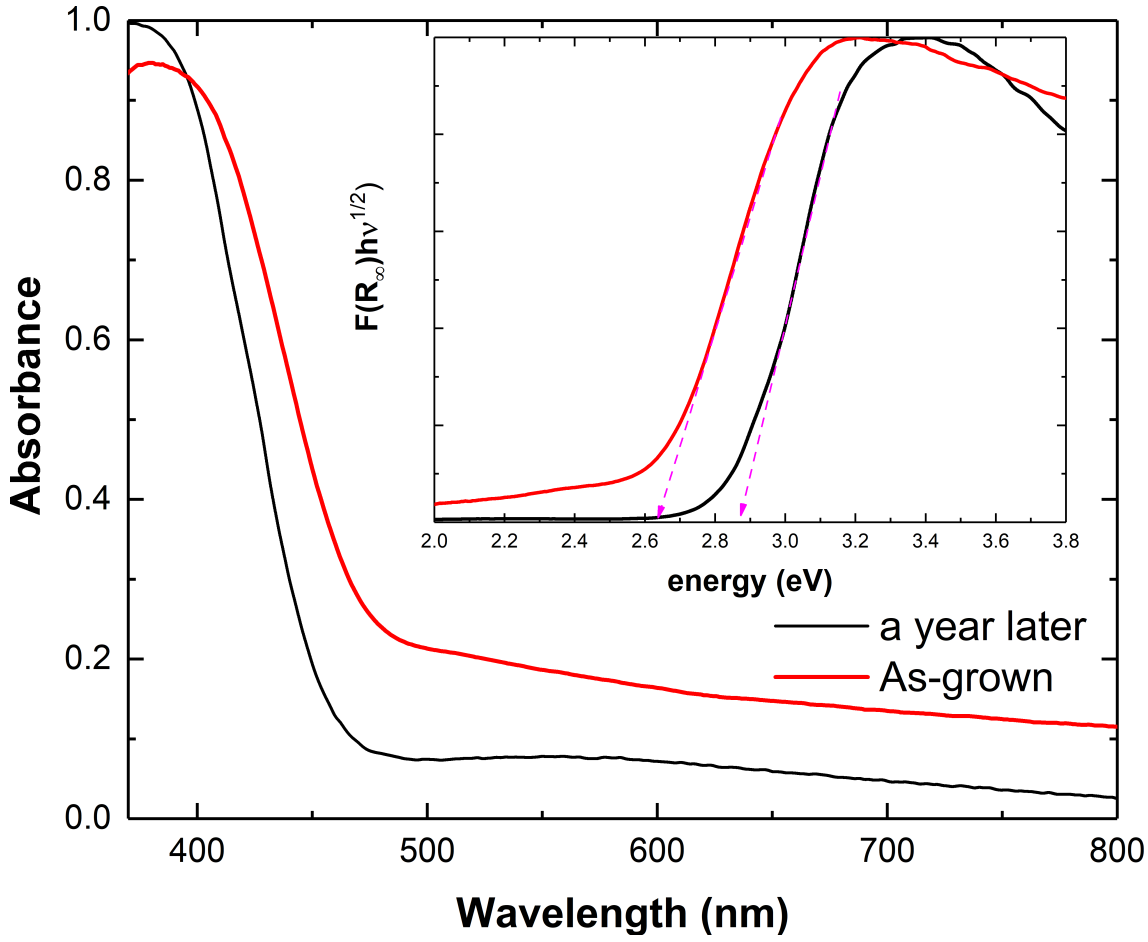

Figure S15 The optical band gap measured for the double perovskite $Cs_2AgSbCl_6$ for as-grown (black line) and 1 year later (red line).

Although the absorbance increased to around 32 nm (see Figure S15), the sample still absorbs in the blue region of the visible spectrum, contributing to its good optoelectronic stability. The notable shift in absorption could be linked to the incorporation of oxygen/water. It is worth noting that after one year of storage (in ambient atmosphere, an average temperature of 27 °C, and relative humidity of 55%), a possible evolution of the $Cs_3Sb_2Cl_9$ phase would be taking place (although not noticed in the PXRD measurement) since the obtained band gap of 2.84 eV is comparable to the value reported in the literature[S7].

References

(S1) Kubicki, D. J.; Saski, M.; MacPherson, S.; Galkowski, K.; Lewiński, J.; Prochowicz, D.; Titman, J. J.; Stranks, S. D. Halide Mixing and Phase Segregation in Cs2AgBiX6 (X = Cl, Br, and I) Double Perovskites from Cesium-133 Solid-State NMR and Optical Spectroscopy. *Chemistry of Materials* **2020**, *32*, 8129–8138, DOI: 10.1021/acs.chemmater.0c01255, PMID: 33071455.

(S2) Ying, P.; Yu, J.; Su, W. Liquid-Assisted Grinding Mechanochemistry in the Synthesis of Pharmaceuticals. *Advanced Synthesis & Catalysis* **2021**, *363*, 1246–1271, DOI: https://doi.org/10.1002/adsc.202001245.

(S3) Friščić, T.; Childs, S. L.; Rizvi, S. A. A.; Jones, W. The role of solvent in mechanochemical and sonochemical cocrystal formation: a solubility-based approach for predicting cocrystallisation outcome. *CrystEngComm* **2009**, *11*, 418–426, DOI: 10.1039/B815174A.

(S4) Rowles, M. R. *pdCIFplotter*: visualizing powder diffraction data in pdCIF format. *Journal of Applied Crystallography* **2022**, *55*, 631–637, DOI: 10.1107/S1600576722003478.

(S5) Lv, K.; Qi, S.; Liu, G.; Lou, Y.; Chen, J.; Zhao, Y. Lead-free silver-antimony halide double perovskite quantum dots with superior blue photoluminescence. *Chem. Commun.* **2019**, *55*, 14741–14744, DOI: 10.1039/C9CC07397C.

(S6) Kubelka, P.; Munk, F. An article on optics of paint layers. *Z. Tech. Phys* **1931**, *12*, 259–274.

(S7) Pradhan, A.; Jena, M. K.; Samal, S. L. Understanding of the Band Gap Transition in Cs3Sb2Cl9–xBrx: Anion Site Preference-Induced Structural Distortion. *ACS Applied Energy Materials* **2022**, *5*, 6952–6961, DOI: 10.1021/acsaem.2c00591.